Inorganic Chemistry

Article

Tritopic (Cascade) and Ditopic Complexes of Halides with an Azacryptand

Md. Alamgir Hossain, Paula Morehouse, Douglas Powell, and Kristin Bowman-James*

Department of Chemistry, University of Kansas, 1251 Wescoe Hall Drive, Lawrence, Kansas 66045

Structural aspects of the binding of halides in the octaaza cryptand (1,4,11,14,17,24,29,36-octa-azapentacyclo-[12.12.12.$2^{6,9}$.$2^{19,22}$.$2^{31,34}$]-tetratetraconta-6(43),7,9(44),19(41),20,22(42),31(39),32,34(40)-nonaene, N(CH$_2$CH$_2$NHCH$_2$-*p*-xylyl-CH$_2$NHCH$_2$CH$_2$)$_3$N), **L**^{1}, were examined for fluoride, chloride, and bromide. Crystallographic results for two different fluoride complexes indicated cascade-like coordination, with two fluoride ions inside the tren-based cavity, bridged by a water molecule. In the two different chloride structures, a single chloride and a water molecule occupied the cavity. The bromide structure contained two crystallographically independent cationic cryptands. Unit A consisted of a bromide on one side of the cavity and three disordered water molecules situated between the cryptand arms on the other side. Unit B also had a bromide inside the cavity at one side, but a single molecule of water was centered at the other side of the cavity. Association constants for the three ions, determined by NMR titrations in aqueous solution at pH 5, revealed log K_a = 3.15(5), 3.37(3), and 3.34(4) for fluoride, chloride, and bromide, respectively.

Introduction

Tremendous strides have been made in elucidating the structural aspects of anion coordination in recent years.[1,2] Many of the findings indicate that there can be striking structural parallels with transition metal coordination chemistry. For example, we have observed ditopic binding of nitrate,[3,4] cascade complexes with fluoride,[5] "sandwich" formation with sulfate,[6] as well as the chelate and macrocyclic effects[3–7] in the stabilization of anion complexes. These similarities can be traced to analogies between the coordinate covalent bonds in transition metal complexes and the hydrogen bonds formed in anion complexes. Further

substantiation of the topological relationship between transition metal and anion coordination chemistry is the isolation of consistent structural motifs for given anions under a variety of conditions.

The term "cascade complex" was coined by Lehn and co-workers,[8,9] who noted that azacryptand ligands often incorporate two metal ions that are linked via a bridging anion (cascade) (Scheme 1A). A number of different monocyclic and bicyclic ligands have been shown to be capable of forming cascade complexes with a variety of metal ions, including Cu^{2+}, Co^{2+}, Ni^{2+}, and Zn^{2+}, along with cascading anions, such as halides and pseudo-halides, hydroxide, carbonate, malonate, perchlorate, and sulfate.[8–15] These same

* Author to whom correspondence should be addressed. E-mail: kbowman-james@ku.edu.

(1) Bianchi, A.; Bowman-James, K.; García-España, E., Eds. *Supramolecular Chemistry of Anions*; Wiley–VCH: New York, 1997.

(2) Special Issue: 35 Years of Synthetic Anion Receptor Chemistry. *Coord. Chem. Rev.* **2003**, *240*.

(3) Mason, S.; Clifford, T.; Seib, L.; Kuczera, K.; Bowman-James, K. *J. Am. Chem. Soc.* **1998**, *120*, 8899–8900.

(4) Clifford, T.; Danby, A.; Llinares, J. M.; Mason, S.; Alcock, N. W.; Powell, D.; Aguilar, J. A.; García-España, E.; Bowman-James, K. *Inorg. Chem.* **2001**, *40*, 4710–4720.

(5) Hossain, A.; Llinares, J. M.; Mason, S.; Morehouse, P.; Powell, D.; Bowman-James, K. *Angew. Chem., Int. Ed.* **2002**, *41*, 2335–2338.

(6) Hossain, M. A.; Kang, S. O.; Powell, D.; Bowman-James, K. *Inorg. Chem.* **2003**, *42*, 1397–1399.

(7) Hossain, M. A.; Llinares, J. M.; Powell, D.; Bowman-James, K. *Inorg. Chem.* **2001**, *40*, 2936–2937.

(8) (a) Lehn, J.-M.; Pine, S. H.; Watanabe, E.; Willard, A. K. *J. Am. Chem. Soc.* **1977**, *99*, 6766–6768. (b) Lehn, J.-M. *Pure Appl. Chem.* **1980**, *52*, 2441–2459. (c) Dietrich, B.; Guilhem, J.; Lehn, J.-M.; Pascard, C.; Sonveaux, E. *Helv. Chim. Acta* **1984**, *67*, 91–104. (d) Lehn, J.-M. *Science* **1985**, *227*, 849–856.

(9) (a) Motekaitis, R. J.; Martell, A. E.; Lehn, J.-M.; Watanabe, E.-I. *Inorg. Chem.* **1982**, *21*, 4253–4257. (b) Motekaitis, R. J.; Martell, A. E.; Dietrich, B.; Lehn, J.-M. *Inorg. Chem.* **1984**, *23*, 1588–1591.

(10) Harding, C. J.; Mabbs, F. J.; MacInnes, E. J.; McKee, V.; Nelson, J. *J. Chem. Soc., Dalton Trans.* **1996**, 3227–3230.

(11) (a) Amendola, V.; Bastianello, E.; Fabbrizzi, L.; Mangano, C.; Pallavicini, P.; Perotti, A.; Lanfredi, A. M.; Ugozzoli, F. *Angew. Chem., Int. Ed.* **2000**, *39*, 2917–2920. (b) Amendola, V.; Fabbrizzi, L.; Mangano, C.; Pallavicini, P.; Poggi, A.; Taglietti, A. *Coord. Chem. Rev.* **2001**, *219–221*, 821–837.

Scheme 1

A

B
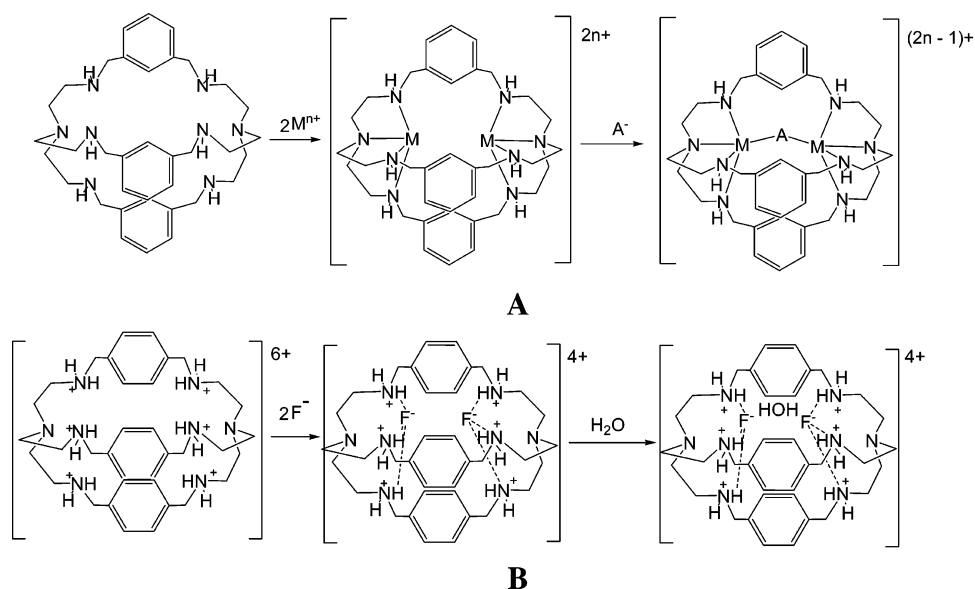
ligands, when protonated, are capable not only of ditopic encapsulation of anionic and neutral species,[3,4,16,17] but also of the formation of cascade complexes,[5] with halides assuming the role of the transition metal ions (Scheme 1B). Herein are reported tritopic cascade and other ditopic modes of halide coordination in an azacryptand with a *p*-xylyl spacer, **L¹**, **1**−**3**. Coordination geometries for the chloride complex and one unit of the bromide complex are quite similar to the structure of the fluoride complex of a somewhat smaller cryptand, **L²**, **4**.[16,17]

1   **2 X = Cl**   **4**
              3 X = Br (Unit B)
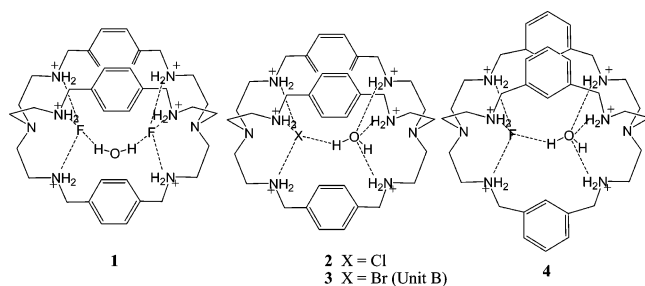
Experimental Section

HF was purchased from Aldrich. Other chemicals were reagent grade and were used without further purification. Elemental analyses were obtained from Desert Analytics, Tucson, AZ. Mass spectral data were obtained from the Mass Spectrometry Laboratory and NMR spectra were recorded using a Bruker AM 500 spectrometer at the NMR Laboratory, both at the University of Kansas.

(12) Harding, C. J.; McKee, V.; Nelson, J.; Lu, Q. *J. Chem. Soc., Chem. Commun.* **1993**, 1768−1770

(13) Menif, R.; Reibenspies, J.; Martell, A. E. *Inorg. Chem.* **1991**, *30*, 3446−3454.

(14) Dussart, Y.; Harding, C.; Dalgaard, P.; McKenzie, C.; Kadirvelraj, R.; McKee, V.; Nelson, J. *J. Chem. Soc., Dalton Trans.* **2002**, 1704−1713.

(15) Drew, M. G. B.; Hunter, J.; Marrs, D. J.; Nelson, J.; Harding, C. *J. Chem. Soc., Dalton Trans.* **1992**, 3235−3242.

(16) Mason, S.; Llinares, J. M.; Morton, M.; Clifford, T.; Bowman-James, K. *J. Am. Chem. Soc.* **2000**, *122*, 1814−1815.

(17) Aguilar, J. A.; Clifford, T.; Danby, A.; Llinares, J. M.; Mason, S.; Garcia-España, E.; Bowman-James, K. *Supramol. Chem.* **2001**, *13*, 405−417.

Synthesis. The macrocyclic cryptand **L¹** was synthesized according to previously published methods and isolated as the free base.[18] ¹H NMR (500 MHz, CDCl₃, TMS): δ 2.67 (t, 12H, NC*H*₂), 2.87 (t, 12H, NCH₂C*H*₂), 3.69 (s, 12H, ArC*H*₂), 6.98 (b, 12H, Ar*H*). ¹³C NMR (125 MHz, CDCl₃, TMS): δ 47.8 (N*C*H₂), 53.4 (NCH₂*C*H₂), 54.1 (Ar*C*H₂), 127.4 (*C*_Ar), 138.4 (*C*H_Ar). FAB-MS: m/z (FAB) 599 [H**L¹**]⁺. Anal. Calcd for C₃₆H₅₄N₈: C, 72.20; H, 9.09; N, 18.71. Found: C, 71.53; H, 8.97; N, 18.61.

[H₆L¹(F)₂(H₂O)][SiF₆]₂·12H₂O, 1. The fluoride complex was obtained by titrating a neutral solution of **L¹** (30 mg, 50 μmol) with a 48% solution of HF to pH 2. A white crystalline powder formed immediately and was recrystallized from *i*-PrOH and H₂O to yield X-ray quality colorless plates. Yield: 45 mg, 78%. ¹H NMR (500 MHz, D₂O, TSP): δ 2.87 (t, 12H, NC*H*₂), 3.31 (t, 12H, NCH₂C*H*₂), 4.25 (s, 12H, ArC*H*₂), 7.43 (d, 12H, Ar*H*). ¹³C NMR (125 MHz, D₂O, TSP): δ 45.0 (N*C*H₂), 48.8 (NCH₂*C*H₂), 51.0 (Ar*C*H₂), 129.8 (*C*_Ar), 131.9 (*C*H_Ar). FAB-MS: m/z 599 [H**L¹**]⁺, 619 [H₂**L¹** ²⁺ + F⁻], 639 [H₃**L¹** ³⁺ + 2F⁻]. Anal. Calcd for C₃₆H₈₀N₈F₁₄O₉Si₂: C, 39.70; H, 7.21; N, 10.28. Found: C, 39.77; H, 7.04; N, 10.23.

[H₆L¹(F)₂(H₂O)][Cl]₂[SiF₆]·10H₂O, (1′). The mixed fluoride/chloride complex was obtained by dissolving **1** (11 mg, 10 μmol) and **2** (9 mg, 10 μmol) in *i*-PrOH (2 mL) with 5 drops of H₂O. Crystals suitable for X-ray analysis were grown in 7 days in a desiccator under the vapor of *i*-PrOH. ¹H NMR (500 MHz, CDCl₃, TMS): δ 2.84 (t, 12H, NC*H*₂), 3.33 (t, 12H, NCH₂C*H*₂), 4.27 (s, 12H, ArC*H*₂), 7.46 (d, 12H, Ar*H*). ¹³C NMR (125 MHz, CDCl₃, TMS): δ 44.6 (N*C*H₂), 49.2 (NCH₂*C*H₂), 51.2 (Ar*C*H₂), 130.0 (*C*Ar), 131.7 (*C*HAr). FAB-MS: m/z 599 [H**L¹**]⁺, 619 [H₂**L¹** ²⁺ + F⁻], 635 [H₂**L¹** ²⁺ + Cl⁻], 639 [H₃**L¹** ³⁺ + 2F⁻], 671 [H₃**L¹** ³⁺ + 2Cl⁻]. Anal. Calcd for C₃₆H₈₀N₈F₈Cl₂O₁₀Si: C, 41.73; H, 7.78; N, 10.82. Found: C, 41.69; H, 7.82; N, 10.78.

[H₆L¹(Cl)(H₂O)][Cl]₅·4H₂O·CH₃OH, 2. The chloride complex was obtained by dissolving **L¹** (30 mg, 50 μmol) in MeOH (2 mL) and adding 6 N HCl (about 200 μL). The white precipitate that formed was redissolved in *i*-PrOH with a few drops of H₂O. Crystals suitable for X-ray analysis were obtained from slow diffusion of MeOH. Yield: 35 mg, 75%. ¹H NMR (500 MHz, D₂O, TSP): δ 2.84 (t, 12H, NC*H*₂), 3.35 (t, 12H, NCH₂C*H*₂), 4.29 (s, 12H,

(18) Chen, D.; Martell, A. E. *Tetrahedron* **1991**, *47*, 6900−6901.

Table 1. Crystallographic Data for $[H_6L(F)_2][SiF_6]_2 \cdot 13H_2O$ (**1**), $[H_6L(Cl)(H_2O)][Cl]_5 \cdot 4H_2O \cdot CH_3OH$ (**2**), and $[H_6L(Br)(H_2O)][Br]_5 \cdot 6.23H_2O$ (**3**)

	1	2	3
empirical formula	$C_{36}H_{86}F_{14}N_8O_{13}Si_2$	$C_{37}H_{74}Cl_6N_8O_6$	$C_{36}H_{74.46}Br_6N_8O$
formula weight	1161.31	939.74	1214.63
crystal system	triclinic	monoclinic	triclinic
space group	$P\bar{1}$	$P2_1/n$	$P\bar{1}$
a (Å)	9.8304(11)	11.4706(6)	10.7509(5)
b (Å)	15.9973(19)	15.7895(9)	19.0486(8)
c (Å)	17.417(2)	27.0054(15)	26.3302(12)
α (deg)	89.959(3)	90.00	107.737(2)
β (deg)	94.633(2)	101.164(2)	101.134(2)
γ (deg)	77.098(2)	90.00	90.680(2)
V (Å^3)	2656.5(5)	4798.5(5)	5024.7(4)
Z	2	4	4
diffractometer	Smart CCD	Smart CCD	Smart CCD
d_{calc} (g/cm^3)	1.452	1.301	1.606
λ (Å)	0.71073	0.71073	0.71073
T (K)	100(2)	100(2)	100(2)
$F(000)$	1232	2008	2457
abs coeff (mm^{-1})	0.180	0.408	4.844
abs corr	semiempirical	semiempirical	semiempirical
max, min trans	0.9632, 0.8936	0.9799, 0.9229	0.7937, 0.2191
θ range	1.67–30.64	1.50–26.00	1.59–30.54
reflns collected	22 911	30 048	42 510
indep reflns	15 608	9438	29 320
R(int)	0.0248	0.0901	0.0333
data/restr/param	15 608/0/655	9438/0/514	28 320/7/1070
$^a R_1$; wR_2	0.0433; 0.1189	0.0449; 0.0873	0.0619, 0.1717
GOF (F^2)	0.974	0.762	1.060

^{a} R_1(obsd data) $= \Sigma||F_o| - |F_c||/\Sigma|F_o|$. w$R_2$ (all data) $= \{\Sigma[w(F_o^2 - F_c^2)^2]/\Sigma[w(F_o^2)^2]\}^{1/2}$.

ArCH_2), 7.47 (d, 12H, ArH). ^{13}C NMR (125 MHz, CDCl$_3$, TMS): δ 44.6 (NCH$_2$), 49.5 (NCH$_2$$CH_2$), 51.2 (Ar$CH_2$), 129.9 ($C_{Ar}$), 131.6 ($CH_{Ar}$). FAB-MS: m/z 599 [H**L**^{1}]$^+$, 635 [H$_2$**L**^{1} $^{2+}$ + Cl$^-$], 671 [H$_3$**L**^{1} $^{3+}$ + 2Cl$^-$], 704 [H$_4$**L**^{1} $^{3+}$ + 3Cl$^-$]. Anal. Calcd for $C_{36}H_{72}N_8$-Cl_6O_6: C, 46.70; H, 7.83; N, 12.10. Found: C, 46.41; H, 7.66; N, 12.16.

[H$_6$L^1(Cl)(H$_2$O)][Cl]$_3$[H$_2$PO$_4$]$_2 \cdot$6.5H$_2$O$\cdot$0.25CH$_3$CH$_2$OH (2′). The mixed Cl/H$_2$PO$_4^-$ complex was obtained from an unsuccessful attempt to prepare a complex of **L^1** with the nucleotide, cytidine 5′-triphosphate (H$_4$CTP). [H$_6$**L^1**][Cl]$_6$ (20 mg, 25 μmol) and Na$_2$H$_2$-CTP (28 mg, 50 μmol) were dissolved in MeOH/H$_2$O/(5:1 v/v, 2 mL), and the solution was kept in a desiccator under MeOH vapor. Crystals suitable for X-ray analysis were isolated after 2 weeks. Due to the small quantity of product, no analytical data were obtained other than the X-ray crystal structure.

[H$_6$L^1(Br)(H$_2$O)][Br]$_5 \cdot$6.25H$_2$O, 3. The bromide complex was obtained by adding 48% HBr (300 μL) dropwise to the free base **L^1** (30 mg, 50 μmol) dissolved in MeOH (2 mL). The white precipitate that formed was collected and washed with Et$_2$O. Recrystallization from MeOH and H$_2$O gave X-ray quality crystals. Yield: 40 mg, 65%. ^{1}H NMR (500 MHz, D$_2$O, TSP): δ 2.83 (t, 12H, NCH_2), 3.33 (t, 12H, NCH$_2$CH_2), 4.28 (s, 12H, ArCH_2), 7.48 (s, 12H, ArH). ^{13}C NMR (125 MHz, CDCl$_3$, TMS): δ 44.5 (NCH$_2$), 49.4 (NCH$_2$$CH_2$), 51.3 (Ar$CH_2$), 129.8 ($C_{Ar}$), 131.6 ($CH_{Ar}$). FAB-MS: m/z 599 [H**L^1**]$^+$, 685 [H$_2$**L^1** $^{2+}$ + Br$^-$], 765 [H$_3$**L^1** $^{3+}$ + 2Br$^-$]. Anal. Calcd for $C_{36}H_{78}N_8Br_6O_6$: C, 36.24; H, 6.54; N, 9.400. Found: C, 36.15; H, 6.48; N, 9.48.

NMR Titrations. ^{1}H NMR titrations of **L^1** with Na$^+$X$^-$ (X$^-$ = F$^-$, Cl$^-$, and Br$^-$) were performed on a Bruker AM500 spectrometer. Samples were prepared in D$_2$O, and initial concentrations were [**L^1**]$_0$ = 2 mM. The pD of the NMR solution was adjusted to 5.0 $\pm$ 0.1 with concentrated solutions of TsOH and NaOD in D$_2$O. A solution of the sodium salt of [2,2,3,3-d_4]-3-(trimethylsilyl)propionic acid (TSP) in D$_2$O in a capillary tube was used as an external reference. All spectra were recorded at room temperature. Each titration was performed by 20–25 measurements using aliquots of

the anion obtained from a 20 mM stock solution. The association constant, K, was calculated by fitting the aliphatic proton signals with a 1:1 association model using Sigma Plot software. The equations used were: $\Delta\delta = ([X]_0 + [L^1]_0 + 1/K - (([X]_0 + [L^1]_0 + 1/K)^2 - 4[L^1]_0[X]_0)^{1/2})\Delta\delta_{max}/2[L^1]_0$. The error limit in K was less than 10%.[19]

X-ray Crystallography. The crystallographic data and details of data collection for **1**–**3** are given in Table 1. Intensity data for all three crystals were collected using a Bruker SMART APEX CCD area detector[20] mounted on a Bruker D8 goniometer using graphite-monochromated Mo Kα radiation (λ = 0.71073 Å). The data were collected at 100(2) K. Intensity data were measured as a series of ω and θ oscillation frames each of 0.3° for times of 5, 45, and 60 s/frame for **1**, **3**, and **2**, respectively. The detector was operated in a 512 × 512 mode and was positioned 5.04 cm from the sample. The coverage of unique data was close to complete (99.4–100%), depending on the sample, out to 26.00° in θ. Cell parameters were determined from a least-squares fit of 2741 reflections in the range 2.22° < θ < 23.92° for **2**, 6474 in the range 2.29° < θ < 30.49° for **3**, and 9504 in the range 2.40° < θ < 30.58° for **1**. Virtually no decay was observed, based on data obtained for a number of peaks monitored at both the beginning and the end of data collection. The data were corrected for absorption by a semiempirical method.[21] Lorentz and polarization corrections were applied, and the data were merged to form a set of independent data for each sample.

Space groups were determined by statistical tests in the triclinic samples, **1** and **3**, and by systematic absences in the monoclinic sample, **2**. The structures were solved by direct methods and refined

(19) Schneider, H.-J.; Kramer, R.; Simova, S.; Schneider, U. *J. Am. Chem. Soc.* **1988**, *110*, 6442–6448.
(20) Data collection: *SMART Software Reference Manual*; Bruker-AXS; Madison, WI, 1994. Data reduction: *SAINT Software Reference Manual*; Bruker-AXS; Madison, WI, 1995.
(21) Sheldrick, G. M. *SADABS*, Program for Empirical Absorption Correction of Area Detector Data; University of Göttingen, Germany, 1996.

Table 2. Hydrogen-Bonding Interactions of Inclusion Species for [H$_6$L(F)$_2$(H$_2$O)][SiF$_6$]$_2$·13H$_2$O (**1**), [H$_6$L(Cl)(H$_2$O)][Cl]$_5$·4H$_2$O·CH$_3$OH (**2**), and [H$_6$L(F)$_2$(H$_2$O)][Cl]$_2$[SiF$_6$]·10H$_2$O (**3**)

1		2	
atoms	distance	atoms	distance
F(1)···H(4B)−N(4)	2.6703(14)	Cl(1)···H(4B)−N(4B)	3.129(3)
F(1)···H(28B)−N(28)	2.6042(14)	Cl(1)···H(28B)−N(28B)	3.167(3)
F(1)···H(33B)−N(33)	2.7237(12)	Cl(1)···H(33B)−N(33B)	3.089(3)
F(1)···H(1SA)−O(1S)	2.7090(13)	Cl(1)···H(1SA)−O(1S)	3.245(2)
F(2)···H(13A)−N(13)	2.6538(14)	O(1S)···H(13A)−N(13)	2.831(3)
F(2)···H(19B)−F(19)	2.6820(14)	O(1S)···H(19A)−N(19)	2.935(3)
F(2)···H(42A)−N(42)	2.6100(14)	O(1S)−H(1SB)···O(2S)	2.727(3)
F(2)···H(1SB)−O(1S)	2.7168(13)		
O(1S)···H(2SA)−O(2S)	2.8886(15)		
O(1S)···H(3SA)−O(3S)	2.8614(15)		

3			
atoms	distance	atoms	distance
Br(1)···H(4A)−N(4A)	3.581(4)	Br(5)···H(13D)−N(13B)	3.350(4)
Br(1)···H(28A)−N(28A)	3.507(4)	Br(5)···H(19D)−N(19B)	3.318(4)
Br(1)···H(33A)−N(33A)	3.433(4)	Br(5)···H(42D)−N(42B)	3.285(4)
Br(1)···H(1SA)−O(1S)	3.203(4)	Br(5)···H(6SA)−O(6S)	3.067(5)
Br(1)···H(2SA)−O(2S)	3.217(4)	Br(5)···H(7SA)−O(7S)	3.237(4)
Br(1)···H(4SB)−O(4S)	3.825(4)		
Br(1)···H(5SA)−O(5S)	3.636(4)		

by full-matrix least-squares methods on F^2.[22] Hydrogen atom positions were initially determined by geometry and refined by a riding model. Non-hydrogen atoms were refined with anisotropic displacement parameters. Hydrogen-bonding interactions of interest for **L**[1] are shown in Table 2.

In the bromide complex, **3**, there was considerable disorder, and two crystallographically distinct hexaprotonated cations were located in an asymmetric unit. For one cation (A), the bromide ion was primarily located at a single side of the macrocycle, with partial occupancy at the other end, refined as 0.971(2) and 0.029(2) (Br(1A) and Br(1B), respectively). One of the external bromides was also disordered, and numbered as Br(13), Br(14), and Br(15). These partial bromides were refined with occupancies of 0.850, 0.107(2), and 0.044(2), respectively. Several water molecules were refined with partial occupancies because of their proximity to bromine positions.

Results and Discussion

Synthesis. The fluoride **1**, chloride **2**, and bromide **3** complexes were all made by titration of the free base in either methanol (fluoride complex) or water (chloride and bromide complexes) with the hydrohalic acid. These reactions were all straightforward, resulting in readily isolable products.

Attempts were also made to synthesize the mixed fluoride/chloride complex from mixing equimolar amounts of the fluoride and chloride complexes, **1** and **2**, respectively. However, this attempt resulted in **1′**, the fluoride cascade with additional chlorides and SiF$_6$$^{2-}$ counterions. Another attempt to isolate a complex with a nucleotide was also unsuccessful. A mixture of **2** and Na$_2$H$_2$CTP in a MeOH/H$_2$O gave a complex with encapsulated chloride and water as in **2** but with three chlorides in addition to two H$_2$PO$_4$$^-$ counterions (instead of CTP) outside of the cavity, structure **2′**. In retrospect, it might have been an anticipated result because nucleotides are known to undergo catalytic hydroly-

sis in the presence of polyammonium macrocycles,[1,2,23] including dien-derived monocycles with aromatic and heterocyclic spacers.[24] However, very early studies of polyammonium receptors indicated only slow hydrolysis of ATP with the bicyclic cryptands.[25] Evidently, the time for crystallization was sufficiently long for hydrolysis to occur. The crystallographic information for **1′** and **2′** is provided in the Supporting Information. The consistency with which the same halide coordination modes for both fluoride and chloride were obtained in the fluoride cascade and the ditopic chloride/water complex lends support to the supposition that these are indeed the preferred coordination geometries for the two anions with **L**[1], and not just accidental coincidences of crystallization.

SiF$_6$$^{2-}$ was identified as one of the counterions in the unit cell for both fluoride-containing complexes, **1** and **1′**. Such an occurrence is common in the presence of fluoride. We have observed this in earlier structures,[16,17] even when efforts are made to keep the reaction mixture from contact with glass containers.

Crystal Structures. [H$_6$L^1(F)$_2$(H$_2$O)][SiF$_6$]$_2$·12H$_2$O (1). The complex crystallizes in the hexaprotonated form, with the cryptand containing two internal fluoride ions (Figure 1). The remaining charge is satisfied by two external SiF$_6$$^{2-}$ counterions. Additionally 13 molecules of water complete the asymmetric unit, including one molecule of water bridging the two fluorides. Extensive hydrogen-bonding networks are observed outside of the cryptand cavity between the macrocycle and the external SiF$_6$$^{2-}$ counterions in **1** and

(22) Sheldrick, G. M. *SHELXTL Version 5 Reference Manual*; Bruker AXS; Madison, WI, 1994. Using *International Tables for Crystallography, Vol. C*; Kluwer: Boston, 1995; Tables 6.1.1.4, 4.2.6.8, and 4.2.4.2.

(23) (a) Mertes, M. P.; Mertes, K. B. *Acc. Chem. Res.* **1990**, *23*, 413−418. (b) Llinares, J. M.; Powell, D.; Bowman-James, K. *Coord. Chem. Rev.* **2003**, *240*, 57−75.

(24) (a) Lu, Q.; Martell, A. E.; Motekaitis, R. J. *Inorg. Chim. Acta* **1996**, *251*, 365−370. (b) Anda, C.; Llobet, A.; Salvado, V.; Reibenspies, J.; Motekaitis, R. J.; Martell, A. E. *Inorg. Chem.* **2000**, *39*, 2986−2999. (c) Anda, C.; Llobet, A.; Salvado, V.; Martell, A. E.; Motekaitis, R. J. *Inorg. Chem.* **2000**, *39*, 3000−3008.

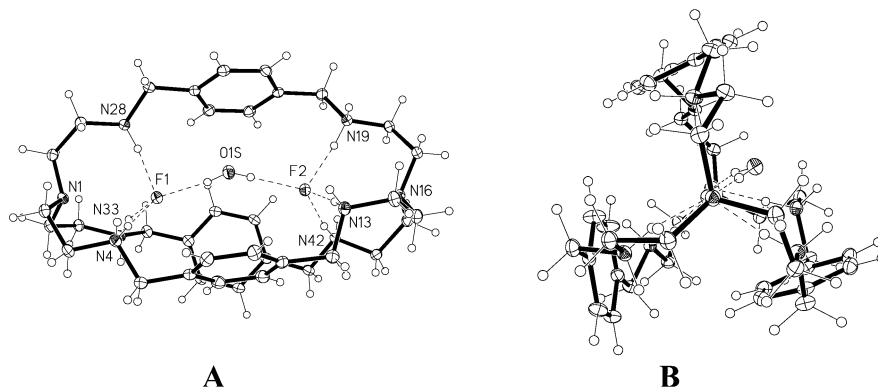(25) Mertes, M. P.; Hosseini, M. W.; Lehn, J.-M. *Helv. Chim. Acta* **1983**, *66*, 2454−2466.

Figure 1. ORTEP drawing of [H$_6$L^1(F)$_2$(H$_2$O)][SiF$_6$]$_2$·12H$_2$O, **1**: (A) side view showing fluoride cascade with water molecule inside the cavity; (B) view down the three-fold axis.

12 water molecules of solvation. We have observed these complex arrays of hydrogen-bonding networks with a number of anion complexes with azacryptands.[3–5,16,17] The structure of **1′** (Supporting Information) is amazingly similar to that of **1** including the short distances between the bridgehead amines and the fluorides.

The span between the bridgehead nitrogens in **L^1** is 10.717 Å. Within the receptor cavity, the two fluorides are slightly displaced from the central axis joining the two bridgehead amines (Figure 1B): 0.124 and 0.229 Å for F(1) and F(2), respectively. The F---F separation is 4.736 Å, and each is almost equidistant from the bridgehead amines at 2.994 and 3.002 Å, slightly less than the van der Waals N---F radius of 3.02 Å.[26] Each fluoride exhibits pseudo-tetrahedral coordination via hydrogen-bonding interactions with three of the secondary ammonium hydrogens and the bridging water molecule (Table 2).

The partially encapsulated oxygen of the bridging water molecule, O(1S), is displaced 1.275 Å from the apical axis. Its pseudo-tetrahedral coordination sphere is completed by hydrogen-bonding interactions with two external water molecules, O(2S) and O(3S), at 2.8886(15) and 2.8614(15) Å, respectively.

The structural features between this and transition metal cascade complexes are quite similar. Many reports of cascade complexes with azacryptands have involved tren-derived complexes with either *m*-xylyl (**L^2**) or furan spacers. In transition metal cascade complexes, the metal is usually considered to be five-coordinate, binding with the trigonally situated neutral amines, and additionally to the bridgehead nitrogen. Dicopper(II) cascades are especially prevalent, and Cu---Cu distances vary considerably. Shorter distances are observed for single anion spacers, such as 3.87 Å for a hydroxo-bridged complex[12] and 4.86 Å for a bromide-bridged cascade[11] in an azacryptand with furan spacers. Longer distances are seen for multiple atom cascades, such as 5.85 Å for a dicopper(II) complex with the **L^2**, first reported by Martell.[13] The structure of this complex was redetermined by Nelson and McKee with different counterions; however, the resulting structure also showed a similar spacing (5.79 Å).[27] To our knowledge, no complete structures have been

reported for cryptands with *p*-xylyl spacers, that is, for **L^1**. An estimate of a Co---Co distance of about 6.5 Å was made from a Patterson function and MM2 calculations in crystals obtained from a cobalt(II) complex with a bridging azide.[15] Suffice it to say, however, that our observed F---F distance of 4.7–4.8 Å is clearly in the range observed for transition metal cascade complexes.

[H$_6$L^1(Cl)(H$_2$O)][Cl]$_5$·4H$_2$O·CH$_3$OH (2). The chloride complex crystallizes with a geometry reminiscent of the fluoride complex with **L^2**, **4**.[16,17] The hexaprotonated ligand **2** contains six chlorides and five water molecules, including the internal chloride and water, as well as a molecule of methanol. As noted for **1**, there tends to be a significant number of hydrogen-bonding interactions between these anion receptor complexes and surrounding water molecules. The molecule of methanol is just outside of the cavity between two of the cryptand arms. The second chloride structure with four chlorides and two dihydrogen phosphate counterions, **2′**, shows the analogous ditopic binding of chloride and water and distances similar to those of **2**.

The internal chloride in **2** is approximately tetrahedrally hydrogen bonded with three of the ammonium nitrogens of a given tren unit and the internal water molecule (Figure 2, Table 2). The chloride and water are farther from the bridgehead nitrogens (3.580 and 3.320 Å, respectively) than in **1**, and considerably farther than the van der Waals radii (3.30 Å for Cl---N and 3.07 Å for O---N).[26] The distance across the cavity (N(1)---N(16)) is 10.093 Å for **2**, somewhat shorter than the 10.717 Å in **1**, as might be anticipated for only two cavity "occupants", as opposed to the tritopic **1** with F–H$_2$O–F guests.

[H$_6$L^1(Br)][Br]$_5$·7.23H$_2$O (3). The bromide complex **3** also crystallizes as the hexahydrobromide but contains two crystallographically independent cationic units. As observed in **1** and **2**, there are again a number of water molecules in the crystal lattice, with extensive hydrogen-bonding interactions interconnecting the various cryptand receptors through water bridges. With regard to the two cationic receptors, one unit (A) contains one bromide ion and three disordered water molecules. The second unit (B) contains one bromide on one

(26) Bondi, A. *J. Phys. Chem.* **1964**, *68*, 441–451.

(27) Dussart, Y.; Harding, C.; Dalgaard, P.; McKenzie, C.; Kadirvelraj, R.; McKee, V.; Nelson, J. *J. Chem. Soc., Dalton Trans.* **2002**, 1704–1713.
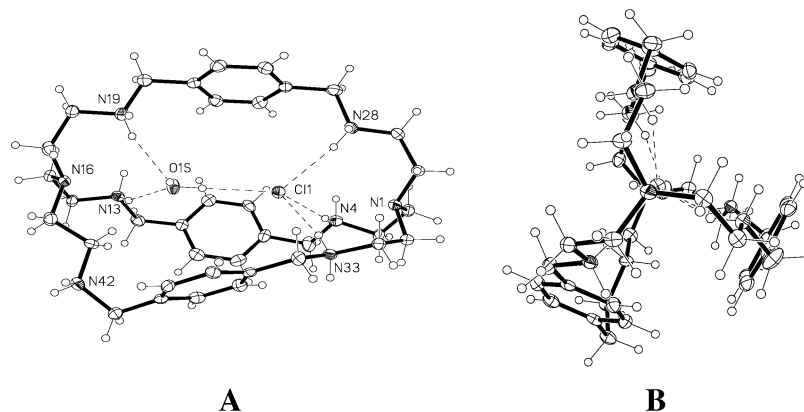
Figure 2. ORTEP drawing of [H$_6$L^1(Cl)(H$_2$O)][Cl]$_5$·4H$_2$O·CH$_3$OH, **2**: (A) side view showing the chloride and water molecule inside the cavity; (B) view down the three-fold axis.

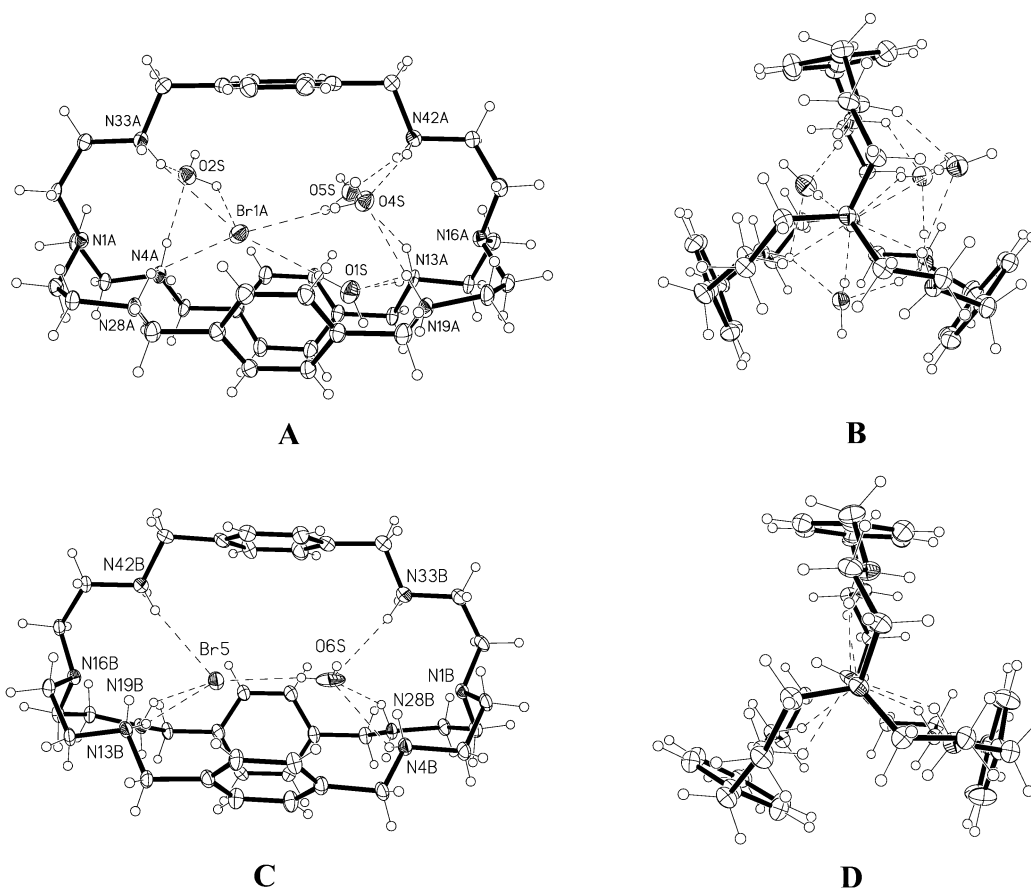**Figure 3.** ORTEP drawing of [H$_6$L^1(Br)(H$_2$O)][Br]$_5$·6.25H$_2$O, **3**: (A) side view showing the bromide and water molecule inside the cavity in unit A; (B) view down the three-fold axis in unit A; (C) side view showing the bromide and water molecule inside the cavity in unit B; (D) view down the three-fold axis in unit B.

side of the cavity and a single water molecule centered at the other side, as observed for the chloride complexes, **2** and **2′**. Because unit B is so similar to the structure of **2**, and because there was considerable disorder around unit A, discussion will first focus on unit B.

The structures of unit B and the chloride complex **2** are very similar (Figure 3C and D). The distances of the bromide and internal water molecule from the bridgehead amines are 3.798 and 3.529 Å, respectively, even longer than that observed for **2**, and in part probably related to the increased size of the bromide. The distance between the bridgehead nitrogens, N(1B)---N(16B), is 10.377 Å. Hydrogen-bonding

distances between Br(5) and the ammonium nitrogens range from 3.285(4) to 3.350(4) Å, and the distance to the internal water is 3.067(5) Å.

In unit A, as noted earlier, there was disorder in the bromide position, with one bromide ion predominant (Br-(1A)) (Figure 3A and B). Again, there is a water molecule in the cavity within hydrogen-bonding distance with the bromide, O(1S) at 3.203(4) Å. A second water molecule is also relatively close to the bromide at 3.217 Å, O(2S), which is situated between N(4A) and N(33A). Two other water molecules lie between the arms of the cryptand, O(4S) and O(5S), but they are considerably farther from the internal
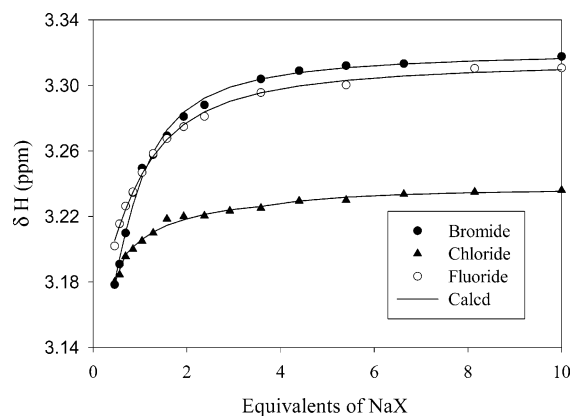
Figure 4. ^{1}H NMR titration curves for the aliphatic signal (NHC*H*$_2$) of L′ with NaX (X$^-$ = F$^-$, Cl$^-$, and Br$^-$) in D$_2$O at 25 °C and pD = 5.0 ± 0.1.

bromide at 3.825(4) and 3.636(4) Å. Whether they should actually be considered as hydrogen bonding with the internal bromide may be questionable. The distance between the bridgehead nitrogens, N(1A)---N(16A), is 10.147 Å, only a little longer than observed for **2**.

NMR. NMR was used for determining the binding constants for both chloride and bromide with **L**^{1}. The binding of fluoride was also previously reported using potentiometric methods,[5] but due to complications of the proximity of the fifth and sixth protonation steps in the presence of chloride and bromide, it was not possible to use this method for these ions. The addition of Na$^+$X$^-$ (X$^-$ = F$^-$, Br$^-$, and Cl$^-$) to the hexatosylate salt of **L**^{1} in D$_2$O at pD 5.0 ± 0.1 caused a downfield shift of the aliphatic proton signals (Figure 4). Negligible shifts were observed for aromatic protons. The NMR titration of **L**^{1} data gave the best fit for a 1:1 binding model of host to guest in all three cases, and yielded log K_a = 3.15(5), 3.37(3), and 3.34(4) for fluoride, chloride, and bromide, respectively. The log K_a for fluoride in the smaller cryptand with the *m*-xylyl spacer, **L**^{2}, under similar conditions is 3.64.[17] The somewhat weaker affinity of fluoride as compared to chloride and bromide in **L**^{1} and fluoride in **L**^{2}

may be a reflection of a poorer fit of the fluoride into the slightly larger **L**^{1} cavity. We did not observe the formation of a binuclear complex at the pH where the measurements were performed, which was higher (5.0 as compared to 2.0) than the pH used to crystallize the cascade complex, **1**.

Conclusions

The isolation and structural characterization of a trinuclear fluoride/water cascade complex in hexaprotonated aza-cryptand **L**^{1} expands the analogies between coordination motifs in transition metal complexes and anion complexes. The characterization of ditopic chloride/water and bromide/water complexes rather than similar cascade tritopic complexes is probably a reflection of the larger anionic radii for these ions, which makes the fit more favorable for just one halide in the cavity. It is especially interesting that this ditopic geometry was also observed for the fluoride complex **4** in the slightly smaller *m*-xylyl-spaced cryptand **L**^{2}.[16,17] The observation of such similar structural patterns in both **2**, **3**, and **4**, including especially the incorporation of water along with the halides, indicates that this is a common binding mode for these systems. It also further substantiates that these hydrogen-bonding geometries are not artifacts of some random binding but actual coordination modes. These findings further expand the understanding of binding topologies in anion coordination chemistry.

Supporting Information Available: Five crystallographic files in CIF format and additional crystallographic data including tables of selected torsion angles, hydrogen bonds, and ORTEPS, including packing diagrams, for all five structures. This material is available free of charge via the Internet at http://pubs.acs.org.

IC048937E